Radiology

ORIGINAL RESEARCH • GASTROINTESTINAL IMAGING

US-based Sequential Algorithm Integrating an AI Model for Advanced Liver Fibrosis Screening

Li-Da Chen, PhD • Ze-Rong Huang, MM* • Hong Yang, PhD • Mei-Qing Cheng, MM • Hang-Tong Hu, MD • Xiao-Zhou Lu, MD • Ming-De Li, MM • Rui-Fang Lu, MM • Dan-Ni He, MM • Peng Lin, MM • Qiu-Ping Ma, MD • Hui Huang, MM • Si-Min Ruan, MD • Wei-Ping Ke, MM • Bing Liao, PhD • Bi-Hui Zhong, PhD • Jie Ren, PhD • Ming-De Lu, PhD • Xiao-Yan Xie, PhD • Wei Wang, PhD*

From the Department of Medical Ultrasonics, Institute of Diagnostic and Interventional Ultrasound (L.D.C., Z.R.H., M.Q.C., H.T.H., M.D. Li, R.F.L., H.H., S.M.R., W.P.K., M.D. Lu, X.Y.X., W.W.), Department of Traditional Chinese Medicine (X.Z.L.), Department of Pathology (B.L.), Department of Gastroenterology (B.H.Z.), and Department of Hepatobiliary Surgery (M.D. Lu), the First Affiliated Hospital of Sun Yat-sen University, No. 58 Zhongshan Rd 2, Guangzhou 510080, People's Republic of China; Department of Medical Ultrasound, the First Affiliated Hospital of Guangxi Medical University, Nanning, People's Republic of China (H.Y., P.L.); Department of Medical Ultrasonics, the Seventh Affiliated Hospital of Sun Yat-sen University, Shenzhen, People's Republic of China (D.N.H.); and Department of Medical Ultrasonics, the Third Affiliated Hospital of Sun Yat-sen University, Guangzhou, People's Republic of China (Q.P.M., J.R.). Received June 13, 2023; revision requested July 31; revision received February 26, 2024; accepted March 1. **Address correspondence to** W.W. (email: *wangw73@mail.sysu.edu.cn*).

This study was funded by National Natural Science Foundation of China (82171960, 82102141), Natural Science Foundation of Guangdong Province (2021B1515020054), Guangdong Regional Joint Foundation (2021B1515120030), and Guangdong High-level Talent Project (0620220202).

* L.D.C. and Z.R.H. contributed equally to this work.

Conflicts of interest are listed at the end of this article.

See also the editorial by Ghosh in this issue.

Radiology 2024; 311(1):e231461 • https://doi.org/10.1148/radiol.231461 • Content codes: GI AI US

Background: Noninvasive tests can be used to screen patients with chronic liver disease for advanced liver fibrosis; however, the use of single tests may not be adequate.

Purpose: To construct sequential clinical algorithms that include a US deep learning (DL) model and compare their ability to predict advanced liver fibrosis with that of other noninvasive tests.

Materials and Methods: This retrospective study included adult patients with a history of chronic liver disease or unexplained abnormal liver function test results who underwent B-mode US of the liver between January 2014 and September 2022 at three health care facilities. A US-based DL network (FIB-Net) was trained on US images to predict whether the shear-wave elastography (SWE) value was 8.7 kPa or higher, indicative of advanced fibrosis. In the internal and external test sets, a two-step algorithm (Two-step#1) using the Fibrosis-4 Index (FIB-4) followed by FIB-Net and a three-step algorithm (Three-step#1) using FIB-4 followed by FIB-Net and SWE were used to simulate screening scenarios where liver stiffness measurements were not or were available, respectively. Measures of diagnostic accuracy were calculated using liver biopsy as the reference standard and compared between FIB-4, SWE, FIB-Net, and European Association for the Study of the Liver guidelines (ie, FIB-4 followed by SWE), along with sequential algorithms.

Results: The training, validation, and test data sets included 3067 (median age, 42 years [IQR, 33–53 years]; 2083 male), 1599 (median age, 41 years [IQR, 33–51 years]; 1124 male), and 1228 (median age, 44 years [IQR, 33–55 years]; 741 male) patients, respectively. FIB-Net obtained a noninferior specificity with a margin of 5% ($P < .001$) compared with SWE (80% vs 82%). The Two-step#1 algorithm showed higher specificity and positive predictive value (PPV) than FIB-4 (specificity, 79% vs 57%; PPV, 44% vs 32%) while reducing unnecessary referrals by 42%. The Three-step#1 algorithm had higher specificity and PPV compared with European Association for the Study of the Liver guidelines (specificity, 94% vs 88%; PPV, 73% vs 64%) while reducing unnecessary referrals by 35%.

Conclusion: A sequential algorithm combining FIB-4 and a US DL model showed higher diagnostic accuracy and improved referral management for all-cause advanced liver fibrosis compared with FIB-4 or the DL model alone.

Supplemental material is available for this article.

Chronic liver disease remains a major global health burden, and liver fibrosis caused by chronic liver disease can lead to cirrhosis, hepatic decompensation, and hepatocellular carcinoma if left untreated (1,2). Liver-related complications can also contribute to further progression of fibrosis (3,4). Screening for advanced liver fibrosis is crucial to enable early diagnosis and treatment.

The screening strategy for liver fibrosis should balance sensitivity to ensure early detection and specificity to minimize false-positive and indeterminate results (5). Liver biopsy, the current reference standard for assessing liver fibrosis, has limited use for screening due to its invasive and costly nature, as well as sampling errors and observer variability (6). As such, various noninvasive tests for assessing liver fibrosis have emerged (5,7). Laboratory tests such as the Fibrosis-4 Index (FIB-4) are easily performed with good reproducibility but lack sufficient sensitivity as a screening tool, especially in discriminating between intermediate stages of fibrosis (8,9). MRI and US elastography are accurate noninvasive tests (10,11). However, these imaging modalities require expensive specialized equipment and experienced

Abbreviations

AUC = area under the receiver operating characteristic curve, DL = deep learning, FIB-4 = Fibrosis-4 Index, LSM = liver stiffness measurement, NPV = negative predictive value, PPV = positive predictive value, SWE = shear-wave elastography

Summary

A sequential algorithm combining the noninvasive tests Fibrosis-4 Index (FIB-4) and a US deep learning (DL) model showed higher diagnostic accuracy and improved referral management for all-cause advanced liver fibrosis compared with FIB-4 or the DL model alone.

Key Results

- In this retrospective study of patients with chronic liver disease or abnormal liver function test results, a US deep learning model (FIB-Net) demonstrated higher specificity (80% vs 61%) for predicting pathologically advanced liver fibrosis compared with the Fibrosis-4 Index (FIB-4) in the internal test set with liver stiffness measurement (LSM) (n = 447).
- A two-step algorithm showed higher specificity than FIB-4 (79% vs 57%) and reduced unnecessary referrals by 42% in the internal and external test sets without requiring access to LSM (n = 1165).

operators, which may not be available in all primary health care settings (12).

Artificial intelligence–based image analysis provides a promising approach for noninvasive assessment of liver fibrosis on US images, offering an accessible tool for primary health care settings (13,14). Although deep learning (DL) algorithms using US images have shown areas under the receiver operating characteristic curve (AUCs) ranging from 0.86 to 0.97 for liver fibrosis detection in several studies (15,16), these studies did not consider how the models could be practically implemented in liver fibrosis screening, which limits their clinical utility.

Indeed, a single noninvasive test may not be adequate to effectively detect the presence of advanced fibrosis. Prior studies have shown a higher positive predictive value (PPV) for two-step (77%) than single-step (55%) strategies (17). However, integrating multimodal medical data to improve diagnostic efficacy remains a challenge (18). Guidelines recommend combining two or more noninvasive tests sequentially to better risk-stratify patients (12,19). Thus, the aim of this study was to develop sequential clinical algorithms that include clinical test data and a US DL model and compare their ability to predict advanced liver fibrosis with that of other noninvasive tests.

Materials and Methods

This retrospective multicenter study received ethical approval from the research ethics committee of each hospital. Because the study was retrospective in nature and images used were fully anonymized, the requirement for informed consent was waived.

Study Sample

The study included patients with a history of chronic liver disease or unexplained abnormal liver function test results who underwent B-mode US of the liver at hospital 1 between January 2014 and July 2022, hospital 2 between January 2019 and December 2019, and hospital 3 between September 2017 and September 2022. The inclusion criteria for the training and validation sets were having undergone both B-mode US and shear-wave elastography (SWE); for the test sets, the inclusion criterion was having undergone liver biopsy. The following patients were excluded: *(a)* those under 18 years of age, *(b)* those with blurred images or the liver parenchyma occupied less than 50% of the US images, *(c)* those with a history of liver transplant or treatment for liver cancer, and *(d)* those with focal liver lesions (except for cysts and calcification foci). Demographic and clinical data were collected.

US Procedure

SWE was used to obtain liver stiffness measurements (LSMs). An Aixplorer US system (SuperSonic Imagine) equipped with an SC6–1 convex probe (frequency range, 1.0–6.0 MHz) was used by radiologists (L.D.C., M.Q.C., and Q.P.M.) with at least 10 years of experience in liver US at hospitals 1 and 2 to obtain the SWE data used in the training and validation data sets (Appendix S1). After patients fasted for 4 hours, measurement was performed in the right lobe of the liver through the intercostal spaces with use of SWE, and large vessels or other moving structures were avoided within the scanning window.

Pathologic Reference Standard

Experienced radiologists who were trained in US-guided liver biopsy performed the procedure (20). The US images were generated using various models of ultrasonic equipment from 11 different manufacturers for testing (Table S1). Similar to SWE examination, the liver biopsy was performed on the right lobe of the liver (Fig S1). Details of liver biopsy and pathologic evaluation are provided in Appendix S2 (21).

Model Development

US-based DL model for predicting liver stiffness.—The fibrosis US-based DL network (FIB-Net) model was developed using the B-mode US segment from the SWE images from hospital 1, which were divided at a 7:3 ratio into a training set and a validation set. External validation of this model was carried out on the B-mode US segment from the SWE data set from hospital 2. B-mode US images in patients diagnosed with advanced fibrosis according to liver biopsy at hospitals 1 and 3 were used as internal and external test sets, respectively, for testing the models' ability to predict advanced fibrosis. There were no overlapping patients between data sets. See Figure 1 for additional details. The workflow of the study is detailed in Figure 2. Image preprocessing is detailed in Appendix S3.

The model was specifically developed to predict whether patients had a liver stiffness value of 8.7 kPa or higher, which indicates advanced fibrosis (≥F3) according to the World Federation for Ultrasound in Medicine and Biology guidelines (22). A deep convolutional neural network architecture (ResNet152) was selected as the classification model and initialized using pretrained weights based on a widely used large-scale image data set (ImageNet). The output of this model was a probability score (less than or equal to the cutoff value means low risk; greater than the cutoff value means high risk). When

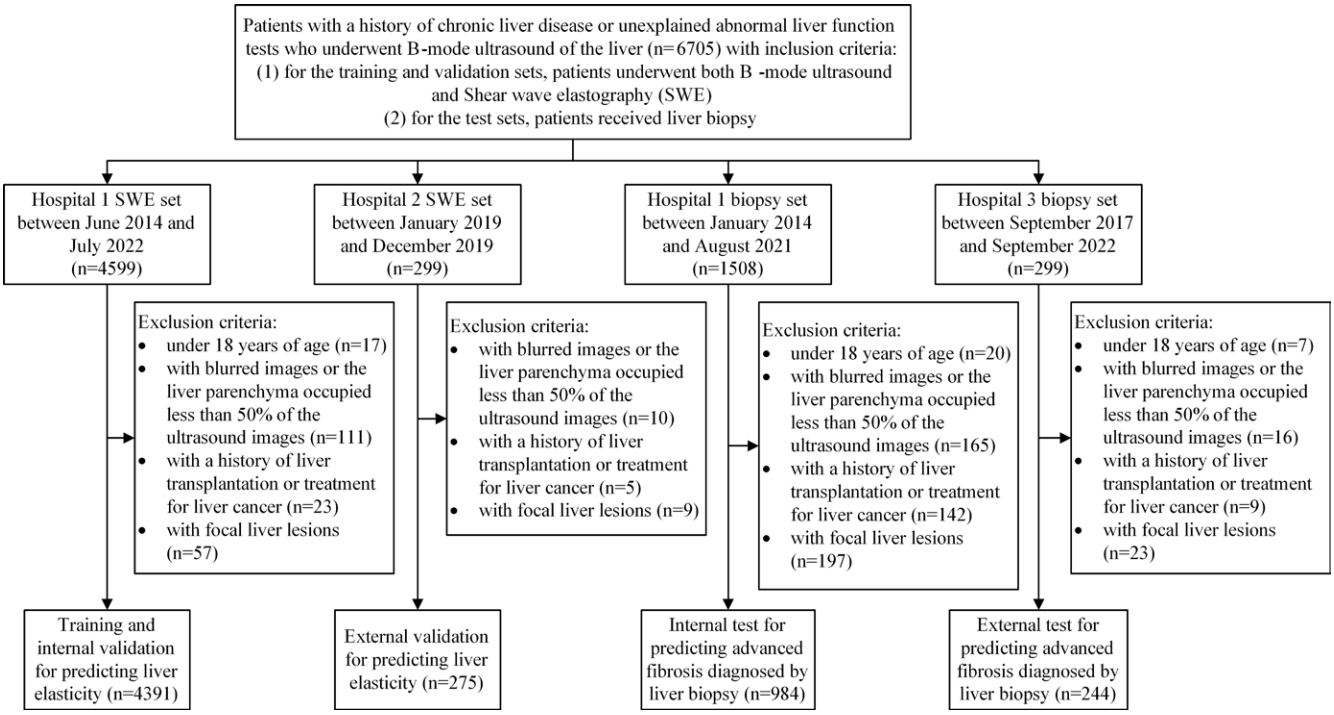

Figure 1: Flowchart of patient inclusion and exclusion criteria for the training, validation, and test data sets. For the hospital 1 biopsy set, 447 had accompanying shear-wave elastography data. Hybrid-Net (a combined US image and patient characteristics model) was developed and tested with the same data sets as the FIB-Net model (a fibrosis US-based deep learning network).

multiple liver images were available for a given patient, the information was consolidated by averaging the predicted probabilities across all images to derive the final predicted score for that patient. Acquisition parameters and model training are detailed in Figures S2 and S3 and Appendix S4. The code is accessible on GitHub *(https://github.com/MedAI-UAIX/FIBNet)*.

Combined US image and patient characteristics model for predicting liver stiffness.—B-mode US images, patient age, and laboratory indexes of aspartate aminotransferase, alanine aminotransferase, and platelet count were combined in a model, Hybrid-Net *(https://github.com/MedAI-UAIX/FIBNet)*, to predict whether the SWE value was greater than or equal to 8.7 kPa (Appendix S4). The same training data set, internal and external validation data sets, and internal and external test data sets used for the FIB-Net model were used to develop and test the Hybrid-Net model. The output of this model was a probability score (less than or equal to the cutoff value means low risk; greater than the cutoff value means high risk).

Clinical Algorithms for Assessing Advanced Liver Fibrosis

Clinical algorithms were created to determine whether multiple tests perform better than single tests for assessing fibrosis risk. FIB-4 was determined according to the published formula (Appendix S5) (23). For clinical scenarios where LSM is not available, two two-step algorithms were developed. First, patients were classified based on their FIB-4. Those with a FIB-4 of 1.3 or higher (Two-step#1) (Fig 3A) or 1.3–3.25 (Two-step#2) (Fig S4A) were further divided into high- or low-risk groups with use of FIB-Net. These algorithms were evaluated using patients with liver biopsy and FIB-4 data from the internal and external test sets. For clinical scenarios where LSM is available, two three-step algorithms were developed in which patients predicted to be at high risk according to FIB-Net were further divided based on their SWE value, with a cutoff of 8.7 kPa or higher indicating high risk of advanced fibrosis (Three-step#1 [Fig 3B] and Three-step#2 [Fig S4B]). These algorithms were evaluated using patients with liver biopsy and SWE data from the internal test set.

Statistical Analysis

The internal and external test sets were used to test the performance of FIB-Net and Hybrid-Net in predicting advanced liver fibrosis, using liver biopsy as the reference standard. The cutoff values of FIB-Net and Hybrid-Net were determined based on the highest Youden index in the internal validation set. AUC was calculated for each model and FIB-4 and compared using the DeLong method. Specificity, sensitivity, accuracy, PPV, and negative predictive value (NPV) were also calculated.

The internal and external test sets divided based on availability of either SWE or FIB-4 data were used to calculate diagnostic accuracy metrics for SWE and FIB-4, respectively, as well as both DL models, the two- and three-step algorithms, and the European Association for the Study of the Liver guidelines, which use FIB-4 followed by LSM (referred to as *SWE value* in this study) (12). The proportion of patients avoiding referral was calculated, and benefits of the sequential algorithms were evaluated by calculating odds ratios of advanced fibrosis detection against other fibrosis

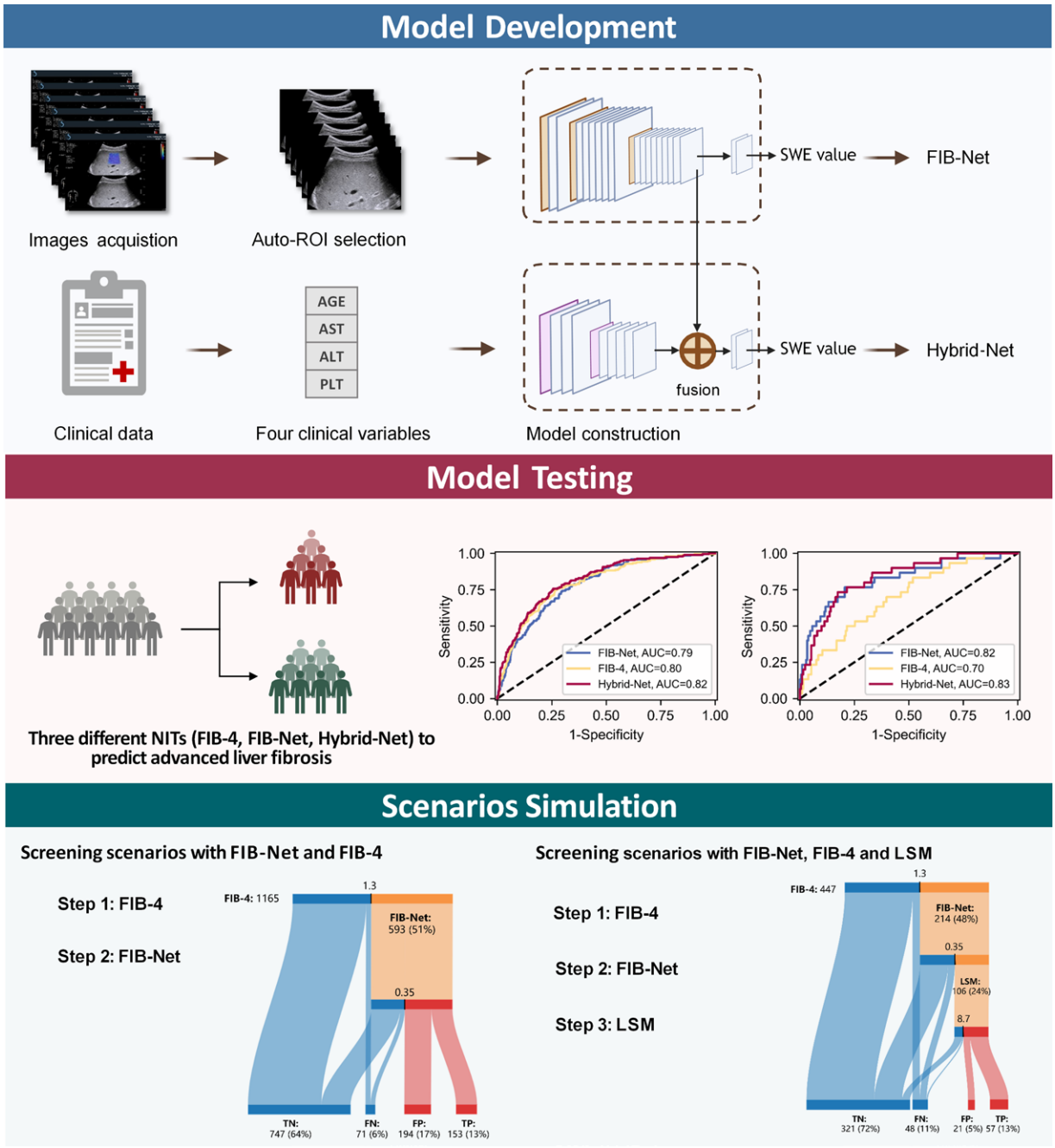

Figure 2: Workflow of the study. B-mode US images and clinical data (age, aspartate aminotransferase [AST] level, alanine aminotransferase [ALT] level, and platelet [PLT] count) were retrospectively retrieved for model development from three health care centers. The developed model, a fibrosis US-based deep learning network (FIB-Net), uses B-mode US images to predict the shear-wave elastography (SWE) value, while Hybrid-Net combines US images and clinical data for the same purpose. The performances of three tests (Fibrosis-4 Index [FIB-4], FIB-Net, and Hybrid-Net) in predicting pathologic advanced liver fibrosis were tested using liver biopsy as the reference standard. Simulations of primary care screening scenarios for diagnosing advanced liver fibrosis in patients with or without liver stiffness measurements (LSMs) were performed. AUC = area under the receiver operating characteristic curve, FN = false negative, FP = false positive, NIT = noninvasive test, ROI = region of interest, TN = true negative, TP = true positive.

assessment tests. The impact of different algorithms on NPV and PPV at varying prevalence of advanced fibrosis was assessed using a previously described method (24) (Appendix S6). In scenarios where the prevalence of advanced fibrosis varied, the predictive values for individual diagnosis were estimated. Subgroup analysis was performed in patients with and without hepatitis B to assess generalizability of the model. Noninferiority analysis of FIB-Net and Hybrid-Net compared with SWE was conducted (Appendix S7). Statistically significant difference was defined as $P < .05$ for all two-sided tests. The statistical analyses were carried out by an author (Z.R.H.) using Python version 3.8 (Python Software Foundation). The justification of sample size is provided in Appendix S8.

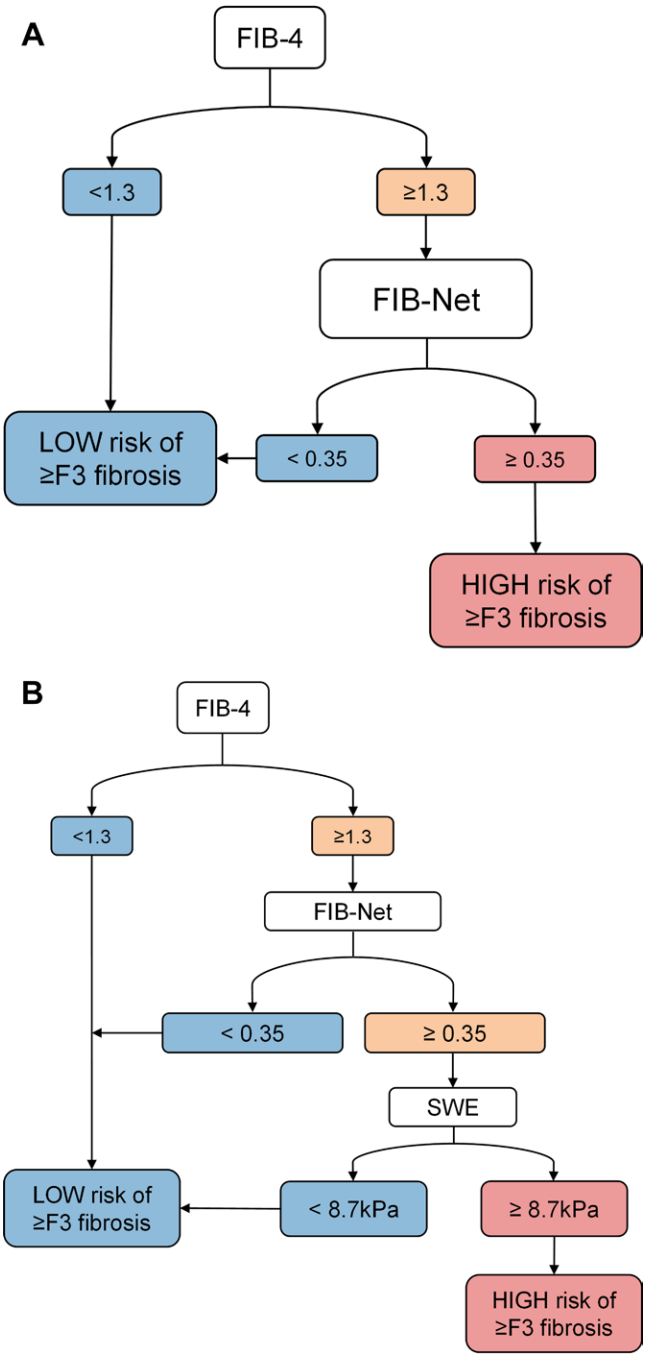

Figure 3: Diagrams show sequential algorithms combining noninvasive tests to detect all-cause hepatic fibrosis. **(A)** For the Two-step#1 algorithm, the first step involves classifying patients into two groups based on their Fibrosis-4 Index (FIB-4). Those with a FIB-4 under 1.3 were considered low risk (<F3), while those with a FIB-4 of 1.3 or higher were further divided into high-risk (probability score cutoff ≥0.35) and low-risk (cutoff <0.35) groups using the developed fibrosis US-based deep learning network (FIB-Net) model as the second step. **(B)** For the Three-step#1 algorithm, the first step involves classifying patients into groups based on their FIB-4. Those with a FIB-4 under 1.3 were considered low risk (<F3), while patients with a FIB-4 of 1.3 or higher were classified using a second-step test of FIB-Net. The high-risk group (FIB-Net cutoff ≥0.35) was further divided based on their shear-wave elastography (SWE) value, where patients with a SWE value of 8.7 kPa or higher were considered at high risk of advanced fibrosis, while the remaining patients were classified as low risk.

Results

Baseline Patients Characteristics

A total of 6705 patients were initially included. Forty-four patients were excluded due to age less than 18 years, 302 due to blurred images or the liver parenchyma occupying less than 50% of the US images, 179 due to a history of liver transplant or treatment for liver cancer, and 286 due to focal liver lesions (Fig 1). Finally, the training and internal validation, external validation, internal test, and external test data sets included 4391 (median age, 42 years [IQR, 33–52 years]; 3000 male), 275 (median age, 43 years [IQR, 34–50 years]; 207 male), 984 (median age, 44 years [IQR, 33–55 years]; 623 male), and 244 (median age, 44 years [IQR, 34–55 years]; 118 male) patients, respectively (Tables 1, S2). The workflow of the study is shown in Figure 2.

Performance of US-based DL Models for Predicting Liver Stiffness in the Validation Data Sets

The cutoff values for FIB-Net and Hybrid-Net were 0.35 and 0.25, respectively. The accuracy of the US-based FIB-Net model was observed to be higher than that of FIB-4 for both the internal (82% [1053 of 1280 patients] vs 74% [951 of 1280]) and external (78% [203 of 261 patients] vs 76% [198 of 261]) data sets (Table S3). The specificity of FIB-4 was lower than that observed for FIB-Net in the internal validation data set (internal, 72% [712 of 985 patients] vs 88% [870 of 985] [P < .001]; external, 81% [154 of 190 patients] vs 84% [159 of 190] [P = .59]). The PPV for both data sets was also higher for FIB-Net than for FIB-4 (internal, 47% [239 of 512 patients] vs 61% [183 of 298]; external, 55% [44 of 80 patients] vs 59% [44 of 75]). The Hybrid-Net model, which combines US images and patient clinical data, achieved the highest AUC for both data sets (internal, 0.89 [95% CI: 0.87, 0.91]; external, 0.85 [95% CI: 0.79, 0.90]) (Fig 4A, 4B; Table S3).

Performance of US-based DL Models for Predicting Pathologically Confirmed Advanced Liver Fibrosis in the Test Data Sets

In the internal test set, the specificity and sensitivity of FIB-Net was observed to be similar to that of FIB-4 (specificity, 63% [457 of 727 patients] vs 60% [433 of 727] [P = .22]; sensitivity, 79% [153 of 194 patients] vs 84% [162 of 194] [P = .30]) (Table 2, Fig 4C). In the external test set, Hybrid-Net showed a higher AUC than that of FIB-4 (0.83 [95% CI: 0.76, 0.91] vs 0.70 [95% CI: 0.61, 0.80]; P = .004) (Fig 4D) as well as a higher specificity (63% [135 of 214 patients] vs 48% [102 of 214]; P = .002) and PPV (25% [26 of 105 patients] vs 18% [25 of 137]) (Table 2). Among patients with available SWE results, FIB-Net and Hybrid-Net obtained noninferior specificity with a margin of 5% (P < .001) compared with SWE (82% vs 80% and 83%, respectively) (Appendix S7).

Evaluation of Clinical Algorithms Including Multiple Tests for Assessing Advanced Liver Fibrosis

Primary care screening without LSM.—Based on the sequential use of FIB-4 and following LSM in European Association for the

Table 1: Clinical Characteristics of Patients in the Data Sets

Characteristic	Training Set		Internal Validation Set		External Validation Set		Internal Test Set		External Test Set	
	SWE Value <8.7 kPa (*n* = 2377)	SWE Value ≥8.7 kPa (*n* = 690)	SWE Value <8.7 kPa (*n* = 1026)	SWE Value ≥8.7 kPa (*n* = 298)	SWE Value <8.7 kPa (*n* = 200)	SWE Value ≥8.7 kPa (*n* = 75)	F0, F1, and F2 (*n* = 781)	F3 and F4 (*n* = 203)	F0, F1, and F2 (*n* = 214)	F3 and F4 (*n* = 30)
No. of images	4622	1362	1994	588	1009	396	2244	631	791	65
Age (y)*	39 (32–49)	51 (43–58)	39 (31–49)	49 (41–56)	40 (33–48)	49 (41–55)	47 (35–56)	54 (45–62)	44 (32–53)	54 (43–60)
Age range (y)	18–84	18–84	18–84	20–84	18–77	30–71	18–79	19–87	18–76	23–72
Sex										
F	808 (34.0)	176 (25.5)	333 (32.5)	74 (24.8)	60 (30.0)	8 (10.7)	299 (38.3)	62 (30.5)	111 (51.8)	15 (50)
M	1569 (66.0)	514 (74.5)	693 (67.5)	224 (75.2)	140 (70.0)	67 (89.3)	482 (61.7)	141 (69.5)	103 (48.1)	15 (50)
Cause of liver disease										
Hepatitis B	1995 (83.9)	616 (89.3)	863 (84.1)	244 (81.9)	161 (80.5)	62 (82.7)	336 (43.0)	156 (76.8)	56 (26.2)	9 (30.0)
Other	382 (16.1)	74 (10.7)	163 (15.9)	54 (18.1)	39 (19.5)	13 (17.3)	445 (57.0)	47 (23.2)	158 (73.8)	21 (70.0)
Fibrosis stage										
F0	NA	NA	NA	NA	NA	NA	343 (43.9)	0 (0)	17 (7.9)	0 (0)
F1	NA	NA	NA	NA	NA	NA	294 (37.6)	0 (0)	117 (54.7)	0 (0)
F2	NA	NA	NA	NA	NA	NA	144 (18.4)	0 (0)	80 (37.4)	0 (0)
F3	NA	NA	NA	NA	NA	NA	0 (0)	93 (45.8)	0 (0)	8 (26.6)
F4	NA	NA	NA	NA	NA	NA	0 (0)	110 (54.1)	0 (0)	22 (73.3)
FIB-4*	0.94 (0.66–1.38)	2.22 (1.42–4.17)	0.94 (0.66–1.35)	2.24 (1.41–4.16)	0.9 (0.6–1.2)	1.6 (1.1–2.8)	1.1 (0.7–1.9)	3.0 (1.6–5.1)	1.39 (0.74–2.50)	2.62 (1.43–5.09)
Patients with SWE value	2377 (100)	690 (100)	1026 (100)	298 (100)	200 (100)	75 (100)	365 (46.7)	103 (50.7)	0 (0)	0 (0)
SWE value (kPa)*	5.7 (5.0–6.7)	12.3 (10.0–16.2)	5.7 (5.0–6.5)	12.1 (10.1–15.9)	5.8 (5.0–6.6)	14.6 (10.1–16.9)	6.4 (5.2–7.9)	13.7 (9.2–22.0)	NA	NA

Note.—Unless otherwise specified, data are numbers of patients, with percentages in parentheses. Fibrosis-4 Index (FIB-4) was calculated according to the formula in Appendix S5. NA = not applicable, SWE = shear-wave elastography.

* Data are medians, with IQRs in parentheses.

Study of the Liver guidelines, the FIB-Net model was included in the clinical algorithms. In patients in the internal and external test sets with liver biopsy but without requiring access to SWE data (*n* = 1165), the Two-step#1 algorithm (ie, FIB-4 followed by FIB-Net) showed higher specificity and PPV than FIB-4 alone (79% [747 of 941 patients] vs 57% [535 of 941] [*P* < .001] and 44% [153 of 347 patients] vs 32% [187 of 593], respectively) (Table 3, Fig 5A). Compared with FIB-4 alone, this algorithm reduced 42% of unnecessary referrals and improved the odds of detection of advanced fibrosis (odds ratio, 1.71 [95% CI: 1.30, 2.25]; *P* < .001) and cirrhosis (1.66 [95% CI: 1.22, 2.27]; *P* = .001) (Table 4). Additionally, compared with FIB-Net alone, the use of the Two-step#1 algorithm resulted in a 35% reduction in unnecessary referrals and increased odds for the detection of advanced fibrosis (odds ratio, 1.53 [95% CI: 1.16, 2.02]; *P* = .003) and cirrhosis (1.49 [95% CI: 1.09, 2.03]; *P* = .02). The results of the Two-step#2 algorithm are provided in Table S4 and Figure S5A.

Primary care screening with LSM.—In patients in the internal test set with liver biopsy and SWE data (*n* = 447), the Three-step#1 algorithm (including FIB-4, FIB-Net, and SWE value) showed higher specificity and PPV than the Two-step#1 algorithm (94% [321 of 342 patients] vs 87% [297 of 342] [*P* = .003] and 73% [57 of 78 patients] vs 58% [61 of 106], respectively) (Table 3, Fig 5B). Compared with the modified European Association for the Study of the Liver guidelines, which also include two steps, the Three-step#1 algorithm reduced unnecessary referrals by 35%, but no evidence of a difference was observed for the odds of detection of advanced fibrosis (*P* = .21) or cirrhosis (*P* = .19) (Table 4). The Three-step#1 algorithm led to a smaller number of false-positive results and thus showed higher PPV than the Three-step#2 algorithm (73% [57 of 78 patients] vs 54% [78 of 144]) (Table S4, Fig S5B).

Subgroup analysis.—In patients with (*n* = 521) and without (*n* = 644) hepatitis B in the test data sets, the sequential algorithms (Two-step#1, Three-step#1) showed higher accuracy (range, 77%–88%) than FIB-4 alone (range, 58%–67%) or FIB-Net alone (range, 64%–81%) (Table S5).

Impact of Fibrosis Prevalence on Predictive Values of Noninvasive Tests

In the test set without requiring access to LSM (*n* = 1165), with increasing prevalence of advanced fibrosis, it was observed that the Two-step#1 algorithm resulted in an increased PPV and a

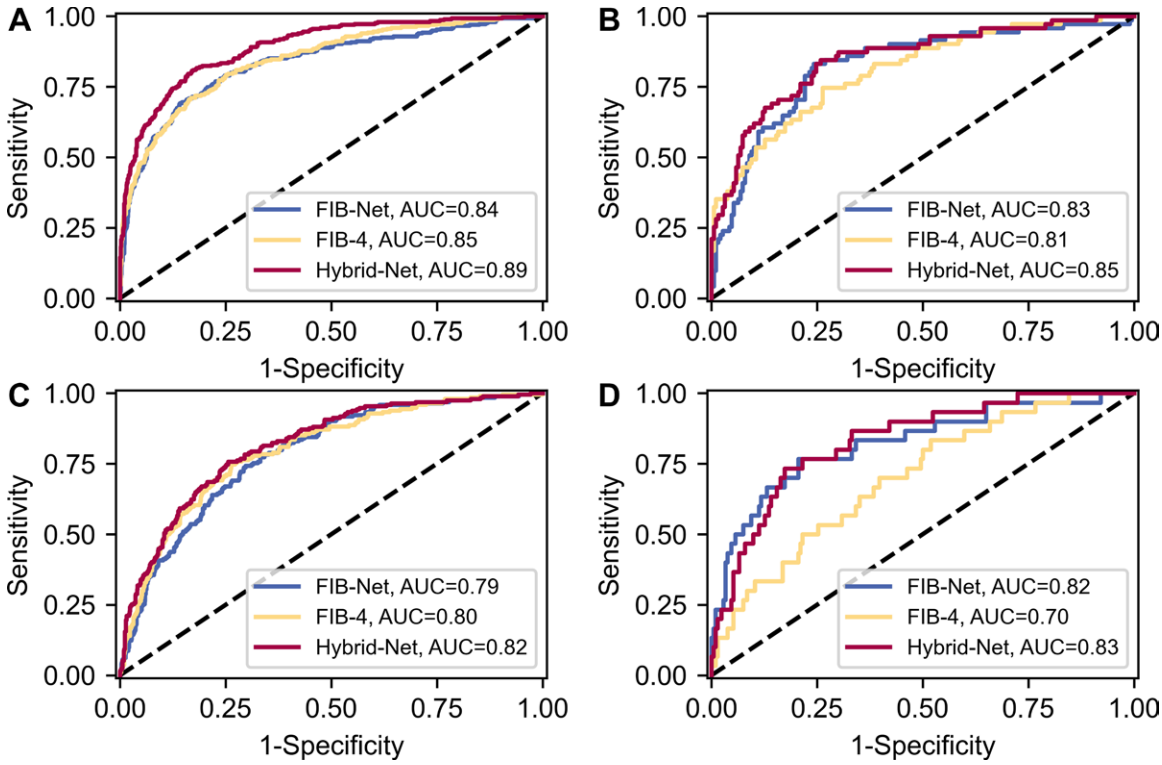

Figure 4: Receiver operating characteristic curves of fibrosis US-based deep learning network (FIB-Net), Fibrosis-4 Index (FIB-4), and a combined US image and patient characteristics model (Hybrid-Net) in the validation and test data sets. **(A)** Receiver operating characteristic curves for each model generated based on patients in the internal validation data set (n = 1280) with available FIB-4 data. **(B)** Receiver operating characteristic curves of each model generated based on patients in the external validation data set with available FIB-4 data (n = 261). **(C)** Receiver operating characteristic curves of each model generated based on patients in the internal test data set with available FIB-4 data (n = 921). **(D)** Receiver operating characteristic curves of each model generated based on patients in the external test data set with available FIB-4 data (n = 244). AUC = area under the receiver operating characteristic curve.

reduced NPV compared with FIB-4 alone (Fig 6A). Between 5% and 20% prevalence, there was a small increase in referral rate (from 18% [214 of 1165 patients] to 26% [302 of 1165]).

In the internal test set with LSM (n = 447), the PPV of the Three-step#1 algorithm reached 86% at 15% prevalence, while at 25% prevalence, the NPV was still 85% (Fig 6B). Details on how the prevalence of advanced fibrosis impacts the Two-step#2 and Three-step#2 algorithms are provided in Figure S6.

Discussion

Noninvasive tests can be used to screen patients with chronic liver disease for advanced liver fibrosis; however, the use of single tests may not be adequate. The aim of this study was to construct sequential clinical algorithms that include a US deep learning (DL) model and compare their ability to predict advanced liver fibrosis with that of other noninvasive tests. The developed US-based DL model (FIB-Net) demonstrated higher specificity (80% vs 61%) and positive predictive value (PPV) (53% vs 38%) for liver fibrosis compared with the Fibrosis-4 Index (FIB-4) in the internal test set with available liver stiffness measurement (LSM) (n = 447). Compared with FIB-4 and FIB-Net alone, a two-step algorithm including both tests showed higher specificity (61% and 80%, respectively, vs 87%) and PPV (38% and 53% vs 58%), reducing unnecessary referrals by 42% in the internal test set with LSM (n = 447).

Previous studies have mainly focused on blood biomarkers (23,25) or liver stiffness estimates to diagnose liver fibrosis (26,27), but these methods are either not suitable for use in clinical practice in patients with all-cause liver disease or may not be available in some clinical settings (28). In contrast, the FIB-Net model developed in this study can use commonly available B-mode US images to assess the staging of all-cause advanced fibrosis, making it more accessible. Although B-mode US images can reflect the degree of liver fibrosis to a certain extent (29,30), extraction of quantitative estimates of liver fibrosis by subjective assessment of the liver remains a challenge. To address this limitation, this study applied a DL approach to quantitatively predict liver stiffness from US images. Compared with other studies (14,31) that have reported AUCs of 0.86–0.92 for models predicting liver fibrosis, the performance of our FIB-Net was lower (AUC, 0.82). We speculated this may be due to the proportion of patients with F4 fibrosis being lower in our study (11%) compared with the other studies, in which 20%–39% of patients had F4 fibrosis. Since we observed that the B-mode US images in patients with cirrhosis have more distinctive features, such as severely heterogeneous liver echogenicity or atrophy, which are easier for a model to detect (29), a higher proportion of patients

Table 2: Performance of FIB-Net and Hybrid-Net for Predicting Pathologically Advanced Liver Fibrosis

Data Set and Fibrosis Test	Threshold	AUC	*P* Value*	Accuracy	Sensitivity	Specificity	PPV	NPV
Internal test set (*n* = 921)								
FIB-4	1.3	0.80 [0.76, 0.83]	…	65 (595/921)	84 (162/194)	60 (433/727)	36 (162/456)	93 (433/465)
FIB-Net	0.35†	0.79 [0.75, 0.82]	.60	66 (610/921)	79 (153/194)	63 (457/727)	36 (153/423)	92 (457/498)
Hybrid-Net	0.25‡	0.82 [0.78, 0.85]	.28	70 (642/921)	79 (154/194)	67 (488/727)	39 (154/393)	92 (488/528)
External test set (*n* = 244)								
FIB-4	1.3	0.70 [0.61, 0.80]	…	52 (127/244)	83 (25/30)	48 (102/214)	18 (25/137)	95 (102/107)
FIB-Net	0.35†	0.82 [0.73, 0.91]	.06	67 (164/244)	83 (25/30)	65 (139/214)	25 (25/100)	97 (139/144)
Hybrid-Net	0.25‡	0.83 [0.76, 0.91]	.004	66 (161/244)	87 (26/30)	63 (135/214)	25 (26/105)	97 (135/139)

Note.—Unless otherwise specific, data are percentages, with numbers of patients in parentheses. Data in brackets are 95% CIs. FIB-Net is a US-based deep learning model for predicting liver stiffness, and Hybrid-Net is a combined US image and patient characteristics model for predicting liver stiffness. AUC = area under the receiver operating characteristic curve, FIB-4 = Fibrosis-4 Index, NPV = negative predictive value, PPV = positive predictive value.

* *P* values are for the comparison of the AUC of FIB-Net or Hybrid-Net with that of FIB-4 and were calculated using the DeLong test.

† The probability score cutoff value with the highest Youden index in the internal validation set for FIB-Net.

‡ The probability score cutoff value with the highest Youden index in the internal validation set for Hybrid-Net.

Table 3: Diagnostic Accuracy Metrics of Different Methods for Assessing Liver Fibrosis in Simulated Primary Care Screening Scenarios Including Patients with Liver Biopsy in the Internal and External Test Sets

Scenario and Fibrosis Test	Threshold	Accuracy	Sensitivity	Specificity	PPV	NPV
Primary care screening without requiring access to LSM (*n* = 1165)						
FIB-4	1.3	62 (722/1165)	84 (187/224)	57 (535/941)	32 (187/593)	94 (535/572)
FIB-Net	0.35*	66 (774/1165)	80 (178/224)	63 (595/941)	34 (178/523)	93 (595/642)
Hybrid-Net	0.25†	69 (803/1165)	80 (180/224)	66 (623/941)	36 (180/498)	93 (623/667)
Two-step#1 (FIB-4 and FIB-Net)	1.3; 0.35*	77 (900/1165)	68 (153/224)	79 (747/941)	44 (153/347)	91 (747/818)
Primary care screening with LSM (*n* = 447)						
FIB-4	1.3	65 (292/447)	78 (82/105)	61 (210/342)	38 (82/214)	90 (210/233)
FIB-Net	0.35*	78 (350/447)	71 (75/105)	80 (275/342)	53 (75/142)	90 (275/305)
Hybrid-Net	0.25†	81 (362/447)	75 (79/105)	83 (283/342)	57 (79/138)	92 (283/309)
SWE value	8.7 kPa	82 (368/447)	82 (86/105)	82 (282/342)	59 (86/146)	94 (282/301)
Two-step#1 (FIB-4 and FIB-Net)	1.3; 0.35*	80 (358/447)	58 (61/105)	87 (297/342)	58 (61/106)	87 (297/341)
Modified EASL guidelines (FIB-4 and SWE value)	1.3; 8.7 kPa	84 (374/447)	70 (74/105)	88 (300/342)	64 (74/116)	91 (300/331)
Three-step#1 (FIB-4, FIB-Net, and SWE value)	1.3; 0.35*; 8.7 kPa	85 (378/447)	54 (57/105)	94 (321/342)	73 (57/78)	87 (321/369)

Note.—Unless otherwise specified, data are percentages, with numbers of patients in parentheses. FIB-Net is a US-based deep learning model for predicting liver stiffness, and Hybrid-Net is a combined US image and patient characteristics model for predicting liver stiffness. EASL = European Association for the Study of the Liver, FIB-4 = Fibrosis-4 Index, LSM = liver stiffness measurement, NPV = negative predictive value, PPV = positive predictive value, SWE = shear-wave elastography.

* The probability score cutoff value with the highest Youden index in the internal validation set for FIB-Net.

† The probability score cutoff value with the highest Youden index in the internal validation set for Hybrid-Net.

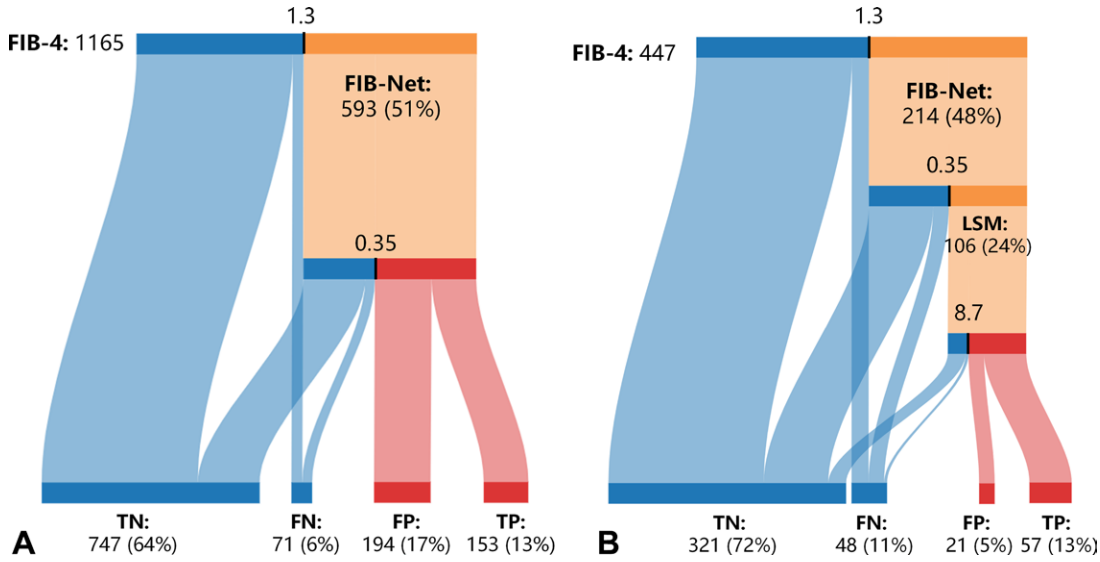

Figure 5: Sankey diagrams show the distribution of true-positive (TP), true-negative (TN), false-positive (FP), and false-negative (FN) results for advanced fibrosis diagnosed using the sequential algorithms. **(A)** Using the combined internal and external data set without requiring access to liver stiffness measurement (LSM) (*n* = 1165) and applying the Two-step#1 algorithm, a Fibrosis-4 Index (FIB-4) under 1.3 was used to rule out patients without advanced fibrosis, and patients with a FIB-4 of 1.3 or higher were further divided into high- and low-risk groups with use of a second-step test of the fibrosis US-based deep learning network (FIB-Net) with a probability score cutoff of 0.35. Of the 1165 patients evaluated using the first step of FIB-4, 593 patients (51%) with a FIB-4 of 1.3 or higher were further evaluated using the second step of FIB-Net, and patients with FIB-Net of 0.35 or higher were given a referral. The true-positive, true-negative, false-positive, and false-negative rates for the Two-step#1 algorithm were 13% (153 of 1165 patients), 64% (747 of 1165), 17% (194 of 1165), and 6% (71 of 1165), respectively. **(B)** Using the internal data set with LSM (*n* = 447) and applying the Three-step#1 algorithm, FIB-4 under 1.3 was used to rule out patients without advanced fibrosis, and patients with FIB-4 of 1.3 or higher were classified using a second-step test of FIB-Net (cutoff: 0.35). The high-risk group was further divided based on their shear-wave elastography (SWE) value, where patients with a SWE value of 8.7 kPa or higher were considered at high risk of advanced fibrosis, while the remaining patients were classified as low risk. Of the 447 patients were evaluated using the first step of FIB-4, 214 of them (48%) had a FIB-4 of 1.3 or higher and were further evaluated using the second step of FIB-Net, 106 of those patients (24%) had FIB-Net of 0.35 or higher and were further evaluated using the third step of SWE, and patients with SWE value of 8.7 kPa or higher were given a referral. The true-positive, true-negative, false-positive, and false-negative rates for the Three-step#1 algorithm were 13% (57 of 447 patients), 72% (321 of 447), 5% (21 of 447), and 11% (48 of 447), respectively.

Table 4: Referral Impact of Sequential Algorithms in the Internal and External Test Sets

Algorithm	Comparator	Referrals Avoided (%)	Advanced Fibrosis or Cirrhosis Detection		Cirrhosis Detection	
			Odds Ratio	*P* Value	Odds Ratio	*P* Value
Two-step#1	FIB-4 ≥ 1.3	42	1.71 (1.30, 2.25)	<.001	1.66 (1.22, 2.27)	.001
Two-step#1	Two-step#2	14	1.16 (0.87, 1.55)	.34	1.16 (0.84, 1.60)	.37
Two-step#1	FIB-Net	35	1.53 (1.16, 2.02)	.003	1.49 (1.09, 2.03)	.02
Two-step#1	Hybrid-Net	28	1.39 (1.05, 1.84)	.02	1.38 (1.01, 1.89)	.04
Three-step#1	FIB-4	77	4.37 (2.47, 7.74)	<.001	3.40 (1.98, 5.83)	<.001
Three-step#1	FIB-Net	59	2.42 (1.33, 4.41)	.004	2.11 (1.20, 3.70)	.01
Three-step#1	SWE value	47	1.89 (1.04, 3.45)	.04	1.80 (1.03, 3.14)	.05
Three-step#1	Hybrid-Net	51	2.03 (1.11, 3.71)	.03	1.84 (1.05, 3.22)	.03
Three-step#1	Two-step#2	55	2.22 (1.21, 4.08)	.01	1.86 (1.05, 3.28)	.04
Three-step#1	Two-step#1	50	2.00 (1.06, 3.76)	.04	1.62 (0.90, 2.93)	.14
Three-step#1	Modified EASL guidelines	35	1.54 (0.82, 2.89)	.21	1.49 (0.83, 2.65)	.19
Three-step#1	Three-step#2	56	2.30 (1.26, 4.18)	.006	1.98 (1.13, 3.45)	.02

Note.—Data in parentheses are 95% CIs. FIB-Net is a US-based deep learning model for predicting liver stiffness, and Hybrid-Net is a combined US image and patient characteristics model for predicting liver stiffness. Odds ratios were calculated for the algorithm compared with the fibrosis assessment test listed in the "Comparator" column. *P* values from χ^2 tests were used to evaluate the statistical significance of differences in odds ratios between the algorithm and comparator. Type I error of the multiple hypothesis tests of the sequential algorithms is likely inflated, necessitating cautious interpretation of significant findings. EASL = European Association for the Study of the Liver, FIB-4 = Fibrosis-4 Index, SWE = shear-wave elastography.

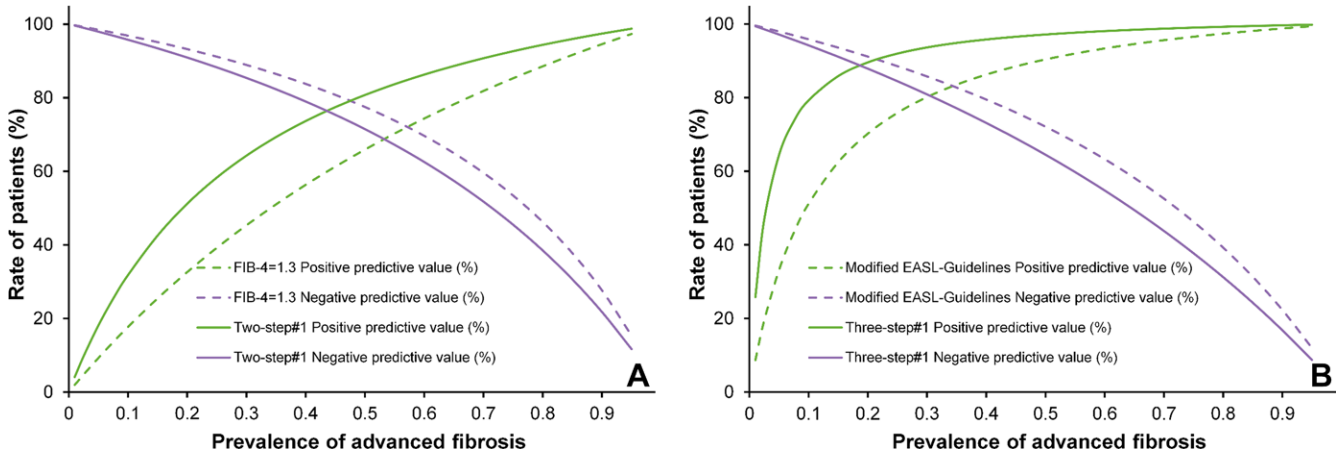

Figure 6: The estimated negative and positive predictive values of different algorithms vary with changes in the prevalence of advanced fibrosis. The green lines correspond to the positive predictive value (PPV) and the purple lines to the negative predictive value (NPV). **(A)** In the test set without requiring access to liver stiffness measurement (n = 1165), the line plot shows the estimated NPV and PPV of the Two-step#1 algorithm (solid lines) and Fibrosis-4 Index (FIB-4) (dashed lines) as a function of the prevalence of advanced fibrosis. With increasing prevalence of advanced fibrosis, the Two-step#1 algorithm resulted in an increased PPV and a reduced NPV compared with FIB-4. With a prevalence of advanced fibrosis at 20%, the PPV for Two-step#1 algorithm is 18 percentage points higher than that of FIB-4 (51% vs 33%), with a 2–percentage point reduction in NPV (91% vs 93%). **(B)** In the internal test set with liver stiffness measurement (n = 447), the line plot shows the estimated NPV and PPV of the Three-step#1 algorithm (solid lines) and modified European Association for the Study of the Liver (EASL) guidelines (dashed lines) as a function of the prevalence of advanced fibrosis. As the prevalence of advanced fibrosis increases, the PPV for Three-step#1 algorithm increases versus the modified European Association for the Study of the Liver guidelines, with a relatively small decrease in NPV. The PPV of Three-step#1 reached 86% at 15% prevalence, while at 25% prevalence, the NPV remains high at 85%.

with F4 fibrosis in previous studies may lead to an overestimation of the model performance.

Our study provides a simulation of a DL model's application in screening scenarios without SWE data in which a two-step algorithm of FIB-4 followed by FIB-Net could be used. In many clinical scenarios, it is common for the first screening step to use a noninvasive test such as FIB-4, and the second step is to triage patients according to a test such as LSM (5,24,32). The specificity of our two-step process (79%) was lower compared with FIB-4 followed by vibration-controlled transient elastography used in the study by Canivet et al (83%) (24), which is justifiable considering that the accuracy of FIB-Net (78%) in detecting advanced fibrosis is not as high as that of LSM (82%). Additionally, our PPV (44%) was lower than that observed in the study by Canivet et al (79%), which can be attributed to the lower proportion of F3 and F4 fibrosis in our study (19%) compared with that in the study by Canivet et al (40%). Regarding the three-step method, our approach demonstrated a specificity comparable to the FIB-4, vibration-controlled transient elastography, and FibroTest approach used in the study by Canivet et al (94% vs 90%), indicating that our three-step approach could serve as a feasible alternative for screening, especially in remote areas where access to advanced medical technology is limited.

Our study included FIB-Net in a sequential algorithmic process rather than directly fusing US image information with clinical data, as has been done in some studies (33,34). Although the fusion network achieved an AUC of 0.90 in the study by Liu, Wen, and Zhu et al (34), our approach focused on reducing referrals and maximizing the efficient use of medical resources.

Our study has limitations. First, the training images were derived from the same transducer and same scanner with SWE. This would limit the robustness of FIB-Net. Second, our limited data set from three centers may restrict the applicability of our results to other populations with varying demographic characteristics, comorbidities, or underlying liver diseases. Third, a comparison between the algorithm using FIB-4 followed by transient elastography and our model could not be performed because the centers involved in this study did not use transient elastography. Finally, type I errors of the sequential algorithms are likely inflated due to multiple hypothesis testing, necessitating cautious interpretation of our findings.

In conclusion, the sequential algorithm combining the Fibrosis-4 Index (FIB-4) and a US-based deep learning (DL) model showed higher diagnostic accuracy and improved referral management for all-cause advanced liver fibrosis compared with FIB-4 or the DL model alone. Future research could focus on validation across patients with different demographic characteristics or causes of liver disease.

Deputy Editor: Kathryn J. Fowler

Scientific Editor: Ariane Panzer

Author contributions: Guarantors of integrity of entire study, **L.D.C., H.Y., M.D. Li, P.L., S.M.R., B.H.Z., J.R., X.Y.X., W.W.**; study concepts/study design or data acquisition or data analysis/interpretation, all authors; manuscript drafting or manuscript revision for important intellectual content, all authors; approval of final version of submitted manuscript, all authors; agrees to ensure any questions related to the work are appropriately resolved, all authors; literature research, **L.D.C., Z.R.H., M.Q.C., H.H., S.M.R., B.L., B.H.Z., X.Y.X., W.W.**; clinical studies, **L.D.C., H.Y., M.Q.C., D.N.H., P.L., Q.P.M., H.H., S.M.R., B.H.Z., J.R., X.Y.X., W.W.**; statistical analysis, **L.D.C., Z.R.H., X.Z.L., M.D. Li, H.H., S.M.R., B.L., B.H.Z.**; and manuscript editing, **L.D.C., Z.R.H., M.Q.C., H.T.H., R.F.L., H.H., S.M.R., B.H.Z., M.D. Lu, W.W.**

Disclosures of conflicts of interest: **L.D.C.** No relevant relationships. **Z.R.H.** No relevant relationships. **H.Y.** No relevant relationships. **M.Q.C.** No relevant relationships. **H.T.H.** No relevant relationships. **X.Z.L.** No relevant relationships. **M.D. Li** No relevant relationships. **R.F.L.** No relevant relationships. **D.N.H.** No relevant relationships. **P.L.** No relevant relationships. **Q.P.M.** No relevant relationships. **H.H.** No relevant relationships. **S.M.R.** No relevant relationships. **W.P.K.** No relevant

relationships. **B.L.** No relevant relationships. **B.H.Z.** No relevant relationships. **J.R.** No relevant relationships. **M.D. Lu** No relevant relationships. **X.Y.X.** No relevant relationships. **W.W.** No relevant relationships.

References

1. Lin CL, Kao JH. Hepatitis B viral factors and clinical outcomes of chronic hepatitis B. J Biomed Sci 2008;15(2):137–145.
2. Parola M, Pinzani M. Liver fibrosis: pathophysiology, pathogenetic targets and clinical issues. Mol Aspects Med 2019;65:37–55.
3. Vergniol J, Foucher J, Terrebonne E, et al. Noninvasive tests for fibrosis and liver stiffness predict 5-year outcomes of patients with chronic hepatitis C. Gastroenterology 2011;140(7):1970–1979, 1979.e1–1979.e3.
4. Sanyal AJ, Van Natta ML, Clark J, et al. Prospective study of outcomes in adults with nonalcoholic fatty liver disease. N Engl J Med 2021;385(17):1559–1569.
5. Ginès P, Castera L, Lammert F, et al. Population screening for liver fibrosis: toward early diagnosis and intervention for chronic liver diseases. Hepatology 2022;75(1):219–228.
6. Bravo AA, Sheth SG, Chopra S. Liver biopsy. N Engl J Med 2001;344(7):495–500.
7. Mózes FE, Lee JA, Selvaraj EA, et al. Diagnostic accuracy of non-invasive tests for advanced fibrosis in patients with NAFLD: an individual patient data meta-analysis. Gut 2022;71(5):1006–1019.
8. Graupera I, Thiele M, Serra-Burriel M, et al. Low accuracy of FIB-4 and NAFLD fibrosis scores for screening for liver fibrosis in the population. Clin Gastroenterol Hepatol 2022;20(11):2567–2576.e6.
9. Lin ZH, Xin YN, Dong QJ, et al. Performance of the aspartate aminotransferase-to-platelet ratio index for the staging of hepatitis C-related fibrosis: an updated meta-analysis. Hepatology 2011;53(3):726–736.
10. Gao Y, Zheng J, Liang P, et al. Liver fibrosis with two-dimensional US shear-wave elastography in participants with chronic hepatitis B: a prospective multicenter study. Radiology 2018;289(2):407–415.
11. Kromrey ML, Le Bihan D, Ichikawa S, Motosugi U. Diffusion-weighted MRI-based virtual elastography for the assessment of liver fibrosis. Radiology 2020;295(1):127–135.
12. European Association for the Study of the Liver; Clinical Practice Guideline Panel; Chair; EASL Governing Board representative; Panel members. EASL Clinical Practice Guidelines on non-invasive tests for evaluation of liver disease severity and prognosis – 2021 update. J Hepatol 2021;75(3):659–689.
13. Meng D, Zhang LB, Cao GT, Cao WM, Zhang GX, Hu B. Liver fibrosis classification based on transfer learning and FCNet for ultrasound images. IEEE Access 2017;5:5804–5810.
14. Lee JH, Joo I, Kang TW, et al. Deep learning with ultrasonography: automated classification of liver fibrosis using a deep convolutional neural network. Eur Radiol 2020;30(2):1264–1273.
15. Anteby R, Klang E, Horesh N, et al. Deep learning for noninvasive liver fibrosis classification: a systematic review. Liver Int 2021;41(10):2269–2278.
16. Dana J, Venkatasamy A, Saviano A, et al. Conventional and artificial intelligence-based imaging for biomarker discovery in chronic liver disease. Hepatol Int 2022;16(3):509–522.
17. Tamaki N, Imajo K, Sharpton SR, et al. Two-step strategy, FIB-4 followed by magnetic resonance elastography, for detecting advanced fibrosis in NAFLD. Clin Gastroenterol Hepatol 2023;21(2):380–387.e3.
18. Fowler KJ, Bashir MR. The current status of imaging in liver fibrosis. Nat Rev Gastroenterol Hepatol 2023;20(10):628–629.
19. Shiha G, Ibrahim A, Helmy A, et al. Asian-Pacific Association for the Study of the Liver (APASL) consensus guidelines on invasive and non-invasive assessment of hepatic fibrosis: a 2016 update. Hepatol Int 2017;11(1):1–30.
20. Rockey DC, Caldwell SH, Goodman ZD, Nelson RC, Smith AD; American Association for the Study of Liver Diseases. Liver biopsy. Hepatology 2009;49(3):1017–1044.
21. Bedossa P, Poynard T. An algorithm for the grading of activity in chronic hepatitis C. The METAVIR Cooperative Study Group. Hepatology 1996;24(2):289–293.
22. Ferraioli G, Filice C, Castera L, et al. WFUMB guidelines and recommendations for clinical use of ultrasound elastography: part 3: liver. Ultrasound Med Biol 2015;41(5):1161–1179.
23. Sterling RK, Lissen E, Clumeck N, et al. Development of a simple noninvasive index to predict significant fibrosis in patients with HIV/HCV coinfection. Hepatology 2006;43(6):1317–1325.
24. Canivet CM, Costentin C, Irvine KM, et al. Validation of the new 2021 EASL algorithm for the noninvasive diagnosis of advanced fibrosis in NAFLD. Hepatology 2023;77(3):920–930.
25. Wai CT, Greenson JK, Fontana RJ, et al. A simple noninvasive index can predict both significant fibrosis and cirrhosis in patients with chronic hepatitis C. Hepatology 2003;38(2):518–526.
26. Martínez SM, Crespo G, Navasa M, Forns X. Noninvasive assessment of liver fibrosis. Hepatology 2011;53(1):325–335.
27. Carrión JA, Navasa M, Forns X. MR elastography to assess liver fibrosis. Radiology 2008;247(2):591–592; author reply 591–592.
28. Kim WR, Berg T, Asselah T, et al. Evaluation of APRI and FIB-4 scoring systems for non-invasive assessment of hepatic fibrosis in chronic hepatitis B patients. J Hepatol 2016;64(4):773–780.
29. Shen L, Li JQ, Zeng MD, Lu LG, Fan ST, Bao H. Correlation between ultrasonographic and pathologic diagnosis of liver fibrosis due to chronic virus hepatitis. World J Gastroenterol 2006;12(8):1292–1295.
30. Iacobellis A, Fusilli S, Mangia A, et al. Ultrasonographic and biochemical parameters in the non-invasive evaluation of liver fibrosis in hepatitis C virus chronic hepatitis. Aliment Pharmacol Ther 2005;22(9):769–774.
31. Ruan D, Shi Y, Jin L, et al. An ultrasound image-based deep multi-scale texture network for liver fibrosis grading in patients with chronic HBV infection. Liver Int 2021;41(10):2440–2454.
32. Fowell AJ, Fancey K, Gamble K, et al. Evaluation of a primary to secondary care referral pathway and novel nurse-led one-stop clinic for patients with suspected non-alcoholic fatty liver disease. Frontline Gastroenterol 2020;12(2):102–107.
33. Gao L, Zhou R, Dong C, et al. Multi-Modal Active Learning For Automatic Liver Fibrosis Diagnosis Based On Ultrasound Shear Wave Elastography. In: 2021 IEEE 18th International Symposium on Biomedical Imaging (ISBI). IEEE, 2021; 410–414.
34. Liu Z, Wen H, Zhu Z, et al. Diagnosis of significant liver fibrosis in patients with chronic hepatitis B using a deep learning-based data integration network. Hepatol Int 2022;16(3):526–536.